Journal of Radiation Research, Vol. 64, No. 2, 2023, pp. 210–227
https://doi.org/10.1093/jrr/rrad002
Advance Access Publication: 11 February 2023

Molecular and cellular basis of the dose-rate-dependent adverse effects of radiation exposure in animal models. Part I: Mammary gland and digestive tract

Keiji Suzuki[1,†,*], Tatsuhiko Imaoka[2,†], Masanori Tomita[3,†], Megumi Sasatani[4,†], Kazutaka Doi[5], Satoshi Tanaka[6], Michiaki Kai[7], Yutaka Yamada[2] and Shizuko Kakinuma[2]

[1]Department of Radiation Medical Sciences, Atomic Bomb Disease Institute, Nagasaki University, 1-12-4 Sakamoto, Nagasaki 852-8523, Japan
[2]Department of Radiation Effects Research, National Institute of Radiological Sciences (NIRS), National Institutes for Quantum Science and Technology (QST), 4-9-1 Anagawa, Inage-ku, Chiba 263-8555, Japan
[3]Biology and Environmental Chemistry Division, Sustainable System Research Laboratory, Central Research Institute of Electric Power Industry (CREIPI), 2-11-1 Iwado Kita, Komae, Tokyo 201-8511, Japan
[4]Department of Experimental Oncology, Research Institute for Radiation Biology and Medicine, Hiroshima University, 1-2-3 Kasumi, Minami-ku, Hiroshima 734-8553, Japan
[5]Department of Radiation Regulatory Science Research, National Institute of Radiological Sciences (NIRS), National Institutes for Quantum Science and Technology (QST), 4-9-1 Anagawa, Inage-ku, Chiba 263-8555, Japan
[6]Department of Radiobiology, Institute for Environmental Sciences, 1-7 Ienomae, Obuchi, Rokkasho-mura, Kamikita-gun, Aomori 039-3212, Japan
[7]Nippon Bunri University, 1727-162 Ichiki, Oita, Oita 870-0397, Japan
*Corresponding author. Department of Radiation Medical Sciences, Nagasaki University Atomic Bomb Disease Institute. 1-12-4 Sakamoto, Nagasaki 852-8523, Japan. Tel: +81-95-819-7116; Fax: +81-95-819-7117; Email: kzsuzuki@nagasaki-u.ac.jp
[†]K. Suzuki, T. Imaoka, M. Tomita and M. Sasatani contributed equally.
(Received 16 April 2022; revised 4 October 2022; editorial decision 9 January 2023)

ABSTRACT

While epidemiological data are available for the dose and dose-rate effectiveness factor (DDREF) for human populations, animal models have contributed significantly to providing quantitative data with mechanistic insights. The aim of the current review is to compile both the *in vitro* experiments with reference to the dose-rate effects of DNA damage and repair, and the animal studies, specific to rodents, with reference to the dose-rate effects of cancer development. In particular, the review focuses especially on the results pertaining to underlying biological mechanisms and discusses their possible involvement in the process of radiation-induced carcinogenesis. Because the concept of adverse outcome pathway (AOP) together with the key events has been considered as a clue to estimate radiation risks at low doses and low dose-rates, the review scrutinized the dose-rate dependency of the key events related to carcinogenesis, which enables us to unify the underlying critical mechanisms to establish a connection between animal experimental studies with human epidemiological studies.

Keywords: radiation; low dose; low dose rate; cell; animal; cancer; epidemiology

INTRODUCTION

The Fukushima Daiichi Nuclear Power Plant accident in 2011 forced much attention to the health effects of exposure to radiation at low dose and low dose-rate. Although it has not been assessed scientifically, from radiation protection point of view, the linear non-threshold (LNT) model has been applied to estimate the cancer risk, which led to multiple layers of unpleasant emotion that makes social problems hindering resilience and recovery of the affected areas [1].

Considering the estimation of cancer risk obtained from the epidemiological studies of atomic-bomb survivors [2, 3], the International Commission on Radiological Protection (ICRP) has applied a reduction value, called the dose and dose-rate effectiveness factor (DDREF), of 2 [4]. The concept relies on the idea that the dose-rate effect is related to the dose response, which is sublinear in the low dose range. Extrapolation of radiation risks estimated at high doses and high dose-rates to low doses and low dose-rates was used to deliver DDREF value.

Inevitably, the DDREF value has been debated by various international organizations, and by the scientists with respect to diverse aspects of emerging novel radiobiological knowledge [5, 6].

Recent studies with animal models have made significant contributions to provide quantitative data and mechanistic insights [7–9]. The application of animal data to human populations remains in debate, but, the information, including the biological mechanisms, is apparently the clue to understand the dose-rate effects of ionizing radiation comprehensively [10, 11]. Thus, the aim of the current review is to compile the animal studies, mostly rodent studies, with respect to the dose-rate-dependent adverse effects. Since intensive discussions have already been carried out elsewhere on the use of animal studies in estimation of the dose-rate effectiveness factor (DREF) [9], the review especially focuses on results with regard to the underlying biological mechanisms of the dose-rate-dependent adverse effects and discussed their possible involvement in the key events related to carcinogenesis.

Recently, utilizing the concept of the adverse outcome pathway (AOP), together with that of the 'key events' leading to an outcome as a clue to the better estimation of radiation risks at low doses and low dose-rates has been discussed [5, 12]. The AOP/key events approach was originally adopted for assessing the risks associated with environmental chemicals [13]. The usage of AOPs has enabled the biology-based estimation of risks from exposure to environmental chemicals, so that the same approach could be useful for radiobiological studies into epidemiology of human populations. In particular, as a systematic representation of current knowledge, the AOP concept is expected to facilitate evaluation of the biological basis of causation from the initial physical events to the cellular and tissue/organ events, and to the individual and population levels [14, 15]. While there are literatures considering the significance of key events in AOP with respect to the dose-rate effects [16, 17], little information is available for animal models. Therefore, we scrutinize the dose-rate dependency of novel key events (Table 1), which should enable unification of the underlying critical mechanisms to connect animal experimental studies with human epidemiological studies.

We selected five tissues/organs, namely the mammary gland, digestive tract, hematopoietic tissue, lung and liver, based upon the higher tissue weighting factor and the amount of available data for the dose-rate effect. The definition of low-dose and low-dose-rate herein follows the consideration by the United Nations Scientific Committee on the Effects of Atomic Radiation (UNSCEAR). An ionizing radiation dose of $<$100 mGy is considered as being low dose, and a dose rate of $<$0.1 mGy/min averaged over 1 h (corresponding to 6 mGy/h) is regarded as low-dose-rate [18].

Typical dose and dose rates used in studies for radiation risk inference by ICRP were recently overviewed by ICRP Task Group 91 [7]. A wide dose-rate range of radiation, from 0.0046 mSv/min of annual effective dose for world population to 7×10^4 Gy/sec of kerma free-in-air for prompt primary gamma radiation at 1000 m from the hypocenter in Hiroshima (assuming a spread in time of the gamma pulse at the ground of 1 ms), was covered. On the other hand, the animal studies considered in this review covered a relatively narrow dose-rate range, which differs from the doses and dose rates considered in the human population studies.

Table 1. AOP and key events

1. Physical/chemical alterations
Ionization and excitation of macromolecules
Ionization of water molecules
2. Biochemical and molecular alterations
DNA damage induction
Chromatin damage induction
Epigenetic changes
3. Molecular and cellular responses
DNA damage repair and responses
Incorrect DNA damage repair
Generation of cancer driver mutations
Intra-cellular signaling
Mitochondria and nuclear DNA
Gene expression & protein production
Cell cycle regulation
Apoptosis, senescence-like cell death, autophagy, necrosis
Non-targeted effects and inter-cellular signaling
4. Tissue/organ responses
Disruption of structure and function of tissues/organs
Alteration of physiology and homeostasis
Stem and progenitor cells
Tissue clearance and stem cell competition
Inflammation and tissue remodeling
Alteration of tissue/organ developments
Development of premalignant regions
5. Adverse outcomes
Induction of cancer
Death from cancer

EPIDEMIOLOGY AND ANIMAL STUDIES

Without doubt, epidemiology is the most important source of information for radiation protection purposes. The greatest advantage of epidemiology is that it examines the human itself, whereas unignorable disadvantages include limitations in the study resulting in various kinds of uncertainties [19–21]. For example, uncertainties in dose and dose-rate, duration and timing limit accurate dose reconstruction. Adverse outcomes are often not directly evaluated, so that failure to ascertain all diseases reduces power, leading to an underestimation of any effect. Furthermore, the possibility of bias could not be excluded, as all possible confounding factors are unable to be considered. In comparison, animal experiments afford greater freedom of design, albeit with the disadvantage that the data acquired are for non-humans. Thus, epidemiology and animal experiments need to be mutually complemented. As listed in Table 2, there are various differences between epidemiology and animal experiments, and these differences must be considered when attempting to make inferences about humans from data of animal studies.

Both epidemiological and animal studies have contributed to the scientific understanding of how dose rate affects health effects of radiation, especially cancer risk. Relevant epidemiological studies include those on nuclear workers (INWORKS [22, 23], Mayak [24] and Million Person Study (MPS) cohorts [25]), environmental exposures

Table 2. Typical differences between epidemiology and animal studies on radiation effects

Item	Epidemiology	Animal study
Target	Human	Non-human
Study design	Many limitations	Free
Population size	Hundreds to millions	Several to thousands
Observation period	Years to decades	Months to years
Identification of disease	Indirect (use of medical and other public registries)	Direct observation
Population homogeneity (genetics, lifestyle, environment, etc.)	Heterogeneous	Homogeneous
Dose/dose rate	Retrospectively estimated	Planned
Age at exposure	Relatively unbiased	Often biased toward young ages
Attained age	Analyzed	Rarely analyzed (due to small sample size)
Effect measures	Relative risk, absolute risk, etc.	Percentage of animals with disease, number of tumors, lifespan, etc.
Statistical analysis	Regression analysis using statistical models	Simple comparisons among groups (in general)
Possibility of confounding	Very high due to life-style factors such as smoking, alcohol consumption	Relatively small because experimental animals are comparatively uniform

(Techa, Chernobyl, High Background Radiation Areas and radioactive fallouts) [20] and medical radiations (tuberculosis, computed tomography scans, etc.) [26]. Nevertheless, the uncertainties inherent to these studies hinder conclusion on whether the cancer risk at low dose rate is smaller than that inferred from studies of acute exposure, such as to atomic-bomb radiation [20]. On the other hand, a large number of experimental studies were reported in the past century and identified generally reduced cancer development in animals exposed at low dose rate as compared with those at high dose rate [8, 27, 28]. More recent efforts have integrated and re-analyzed archived data of such studies [29–31]. In this regard, it would also be meaningful to integrate recent large low-dose-rate exposure experiments conducted at the Institute of Environmental Sciences [32] with comparable high dose rate experiments. Results of animal experiments on specific tissues will be summarized in the following section.

Animal experiments require extrapolation to human, as extensively discussed previously [33]. Comparative studies have shown astonishing concordance among mice, beagle dogs and humans in the dose-dependence of the survival curves [34–36]. Integration of biological and epidemiological findings has been accordingly attempted by BEIR VII (2006) for risk estimation in humans [25]. Furthermore, recent discussions have proposed the idea of integrating epidemiology and biology using the concept of AOP [19] and a 'parallelogram' approach [37] (Fig. 1). Animal experiments are thus considered to be a rich source of information in order to make inferences about radiation effects in humans. Nonetheless, care should be always taken with respect to biological differences between human and experimental animals. For example, frequent tumors in mice often include thymic lymphoma, histiocystic sarcoma and tumors of the pituitary, ovary and Harderian gland, whereas human organs most relevant to radiation protection are the stomach, lung, colon, female breast and bone marrow, followed by liver, bladder, esophagus and thyroid. Ovarian tumors and thymic lymphomas show prominent dose-rate effects,

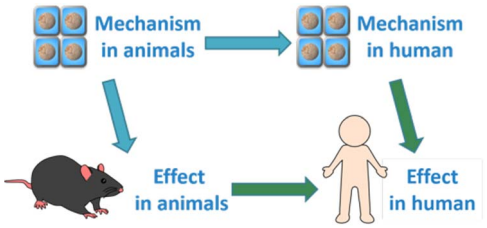

Fig. 1. Parallelogram approach to the integration of epidemiology and animal experiments. The concept of NCRP commentary No. 24 was applied to animal experiments [37].

although the indirect mechanisms for the induction of these tumors, which are irrelevant to human, impede extrapolation to humans [19]. Aging is also species dependent; some attempts have been made to compare human and animal ages in terms of their systemic physiology [38, 39], although more elaborate comparisons should be made for each tissue, like what is done on brain development [40]. Understanding the species difference in physiology and pathogenesis of individual organs is thus crucial for consideration of the applicability of findings from animal studies to human.

STUDIES TOWARDS UNDERSTANDING THE MECHANISMS UNDERLYING DOSE-RATE EFFECTS

To gain mechanistic insights into dose-rate effects it is critical to overview both *in vitro* and *in vivo* studies with respect to the fundamental mechanisms. Thus, this section specifically extracts *in vitro* experiments towards the initial critical key events, i.e. induction of DNA double-strand breaks (DSBs) and mutations, and attempts to rephrase the interpretation of the results.

Summary of *in vitro* studies

Induction of DSBs in cells at low dose

Several previous studies that have investigated dose-rate effects on DSB induction, all of which showed linear dose-dependent induction of DSBs at high doses and high-dose-rates. Although it was rather difficult to quantify the number of DSBs induced by low-dose radiation exposure at a low-dose-rate, it is now possible through the application of surrogate markers for DSBs. This is because such DSB markers are sensitive enough to detect even a single DSB within a cell [41]. Among surrogate DSB markers the foci of phosphorylated histone H2AX at serine 139, called γ-H2AX foci, appear to be the earliest one and used widely in such studies [42]. Since ATM-dependent phosphorylation of histone H2AX expands over several megabases of chromatin [43], phosphorylation is detectable as discrete dots, which are called foci, under a microscope [41], by using a specific monoclonal antibody [44, 45]. There are other DNA damage repair and response factors, which can serve as the markers for DSBs as well [46, 47].

The linear dose–response of γ-H2AX foci was evident between 1.2 mGy and 2 Gy delivered at a high-dose-rate in normal human cells [48], which was confirmed by others [46, 49]. It was claimed that DSBs induced by very low doses were more repairable than those induced by higher doses [48]. For example, the excess amount of DSBs induced by 5 mGy or 20 mGy of X-rays was found to decrease significantly within 24 h after X-irradiation. Similar efficient repair of DSBs caused by low-dose γ-rays was reported elsewhere [49].

DSBs induced at a low-dose-rate radiation

To investigate continuous low-dose radiation exposure, unique radiation exposure facilities have been established [50]. For example, the effects of high- (1.8 Gy/min) and low- (0.3 mGy/min) dose-rate radiation exposure were compared [51]. Whereas exposure to high-dose-rate radiation led to a linear increase in γ-H2AX foci, the same total dose, delivered at low-dose-rate, showed a very small increase within the first 2 days. Another study indicated that, during the 4-days irradiation, the accumulation of foci was observed from day 2 to 4 only by exposure at 0.694 mGy/min not at 0.007, 0.069 and 0.347 mGy/min [52], indicating the balance between the induction of DSBs and their repair is crucial.

As discussed previously, a single DSB has little ability to cause large-scale genome rearrangement, which is one of the critical events leading to cancer [53]. Therefore, even with the same total dose, dose delivered at high-dose-rate can induce multiple DSBs simultaneously in the same cell. In contrast, the same dose but delivered at low-dose-rate can result in spatially and temporally isolated DSBs in different cells, indicating the DREF value should be more than 1. It is well documented that DSBs caused by low-linear energy transfer (LET) radiation are efficiently repaired, although it is also claimed that even a single DSB may be accompanied by a cluster of DNA damage including single-strand breaks and base damage [54]. Furthermore, the possibility that a single radiation track causes two or more DSBs in close proximity has been raised. Such possibility still remains to be explored [55].

Detection of DNA double strand breaks in vivo

Applications of foci of γ-H2AX and 53BP1 have also been attempted in animal studies [56–59]. It was found that 10 mGy of X-rays delivered at 2 Gy/min increased 53BP1 foci as well as γ-H2AX foci in the heart, small intestine and kidney [56]. The reduction in the excess foci indicated that the induced DSBs were reparable when mice were exposed to 100 mGy, while those induced by 10 mGy decreased slightly but not completely even after 72 h of irradiation [58]. Therefore, 10 mGy daily irradiation repeated up to 50 times did not change the focus levels in enterocytes, but resulted in the accumulation of foci in cortical neurons, skin keratinocytes and hair follicles. Thus, even at low dose, DSBs accumulated in tissues, when radiation was delivered at 2 Gy/min.

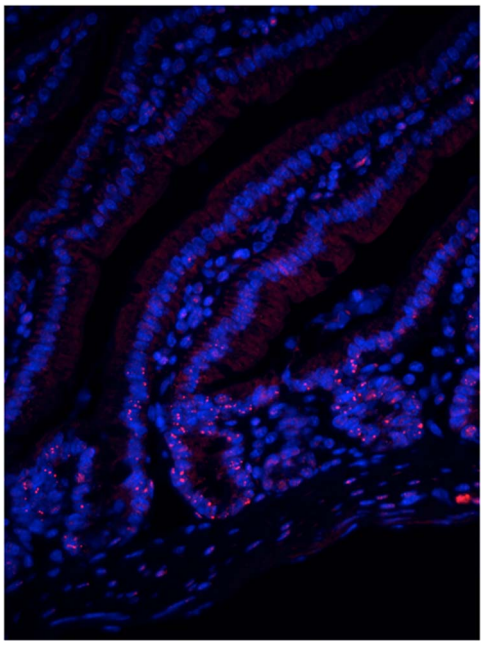

Fig. 2. 53BP1 foci in the mouse small intestine 6 h after 4.0 Gy of X-rays. Multiple foci were induced in the crypt region, while they were rarely detected in villi, indicating that, although DSBs should be induced in every cell, but the DNA damage response, i.e. accumulation of 53BP1, is dependent on differentiation status.

Accumulation of DSBs by continuous irradiation at a very low-dose-rate was examined by using mice in cages were kept on the flood phantom filled with ^{125}I-containing buffer [60]. The low-dose-rate was 0.0017 mGy/min (2.4 mGy/day), while high-dose-rate used was 71 mGy/min and the total dose was 105 mGy, Detectable increase in DNA damage was observed at 71 mGy/min but not at 0.0017 mGy/min [60].

Foci formation was sometimes not apparent in tissues/organs. For example, the human skin basal layers showed focus, while the granular and cornified layers did not develop foci [47]. Similar results were obtained in lung, liver and intestine [58, 59]. Although limitations of sensitivity of detection systems using surrogate markers should be considered, the focus formation was undetectable in heterochromatinized nuclei in terminally differentiated cells [47]. For example, small intestinal crypt cells are highly efficient in inducing foci, which was gradually decreased in the villous regions (Fig. 2). These results clearly demonstrate that activation of DNA damage response, which results

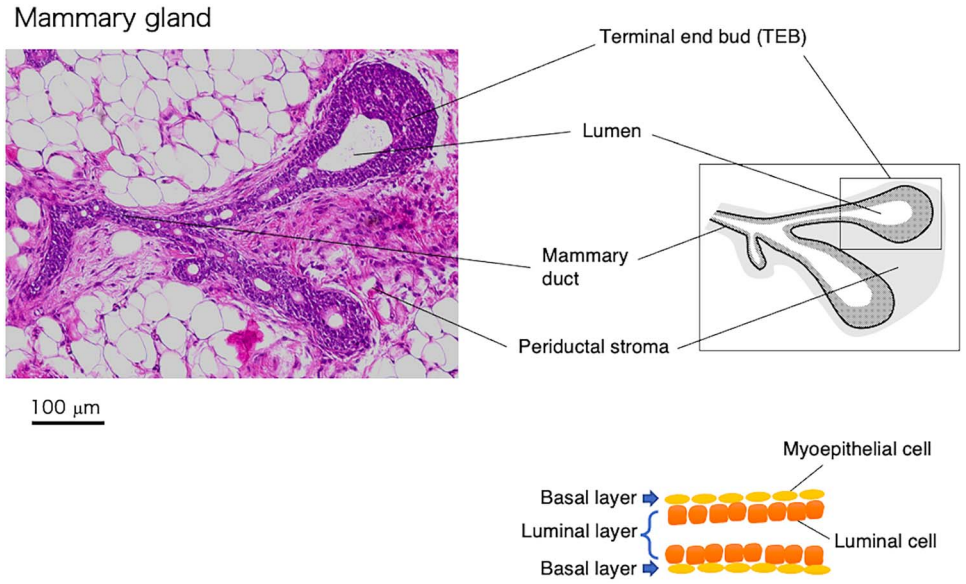

Fig. 3. Architecture of rodent mammary gland.

in the foci formation, is not executed in terminally differentiated cells. Thus, from the biological point of view, a certain fraction of cells in tissues/organs, such as terminally differentiated cells, could not be the cell origin of cancer. Under the low-dose-rate exposure situation, exposed cells may undergo differentiation before the total accumulated dose is delivered, providing one possible mechanism for dose-rate effects *in vivo*.

Summary of knowledge acquired from animal models of cancer development

Large scale animal experiments have defined the dose- and dose-rate-dependency of cancer induction, and more recently, mechanistic insights at the molecular levels, such as DNA damage induction, DNA damage repair and DNA damage response, which are the closely related issues to radiation carcinogenesis, are discussed in detail with respect to genomic instability and mutagenesis [61]. Thus, this section reviews dose-rate effects in animal experiments concerning bone marrow, mammary gland, digestive tract, lung and liver and discusses the possible underlying mechanisms with respect to AOP.

Mammary gland

Breast cancer is the most common malignancy in women. Epidemiological studies such as those on atomic bomb (A-bomb) survivors have demonstrated that radiation exposure is its major risk factor, and increased risk related with radiation dose and the age at exposure [62].

Architecture, development and maintenance. The mammary gland is a tree of branching ducts, consisting of an outer layer of basal (myoepithelial) cells and inner layer of luminal cells (Fig. 3). Species differences does exist between rodents and humans in terms of architecture [63, 64]. In rodents, mammary ducts end in either terminal end buds ([TEB] sites of post-pubertal ductal elongation), terminal ducts and lobuloalveolus and the intra-lobular stroma is scanty (Fig. 3). In humans, mammary ducts end in the terminal ductal lobular unit (TDLU) with rich fibroblastic stroma. The human TDLU is a site at which breast cancer frequently develops and is considered as comparable to the lobuloalveolus and TEBs of rodents [63, 64]. In mice, the fetal gland consists of bipotent cells (i.e. capable of giving rise to basal and luminal lineages), which after birth turn into lineage-restricted basal and luminal progenitors that independently maintain the gland, with some controversial evidence has suggested the existence of long-term bipotent stem cells in adulthood [65]. In rodents, most of the mammary epithelial cells are produced during the post-pubertal development at TEB, which after maturation differentiate into either terminal ducts or lobuloalveolar buds in rodents [64]. Lobuloalveoli undergo extensive growth during pregnancy and lactation, and cessation of lactation induces their involution and remodeling in rodents, a change which is rather mild in human [65].

Mammary epithelial cells undergo cyclic waves of proliferation and death in association with menstrual (~28 days, human) and estrous (4–5 days, mice and rats) cycles [66–68]. In both mice and rats, the progeny of proliferative cells, detected via intense labeling after a few weeks' administration of bromodeoxyuridine, was found to steadily decrease with time and reach one tenth after ~2 months [69, 70], whereas in mice, basal and luminal progenitor cells continue to exist at least for 10 weeks [71, 72], indicating longer life of progenitor cells than differentiated cells. Life of mammary cells in human is not understood.

As ovarian hormones direct development of mammary gland, they also play key roles in mammary carcinogenesis. Early menopause is associated with reduced breast cancer risk in women, and in both rodents and human, high radiation dose (over 2–5 Gy) to ovaries has been associated with early ovarian dysfunction and a reduction in radiation-associated breast cancer risk [73–75]. The effect on the ovary is lower at a low dose rate [76].

Dose-rate effect in radiation carcinogenesis. A series of experimental studies with rats and mice have been conducted. Data obtained from the

comparison between the high dose-rate and low dose-rate exposure have provided rather conflicting results [77–88] (Table 3). It seems likely that dose-rate effects are affected by physiological factors. In fact, continuous administration of estrogen was reported to uncover dose-rate effects [83], consistent with the more recent finding that the dose-rate effect is more prominent in post-pubertal than peri-pubertal rats [76].

Possible 'key events' related to the dose rate effect. As mentioned below, studies have analyzed tissue response of mammary gland to acute single irradiation at a high dose rate. Evidence on early key events in the AOP (Table 1) suggests induction of imbalance between basal and luminal cells as a result of their differential sensitivity to radiation [89], which may be more prominent at high acute doses, providing a possible basis for dose-rate effects. Regarding later key events, stimulation of long-term cell proliferation has been observed after acute radiation exposure, indicating hormonal and microenvironmental alterations. In fact, some microenvironmental changes show a switch-like dose response with a very low threshold, providing another mechanistic basis for the dose-rate effects. Early responses and later tissue kinetics after low dose-rate exposure, including the existence of radiation-induced cell competition [90], remain an open question.

DNA damage responses. γH2AX foci are formed at 1 h, and mostly disappear by 4 h, after a single high-dose (2–6 Gy) irradiation in basal and luminal mammary cells of BALB/c mice, Sprague–Dawley rats and human tissue xenografts and the response is generally more prominent in luminal than basal cells [91–93], although these studies did not conclude whether this also holds true for TEBs and TDLU. γH2AX induction in luminal progenitor cells and mature cells is similar and dose dependent in rats [93]. Basal cells might have high non-homologous end joining (NHEJ) activity in BALB/c mice [92], although, controversially, they are prone to radiation-induced cell death as mentioned below. Focus formation of Rad51 was not detected in irradiated human mammary tissue xenograft, indicating a minor role for homologous recombination (HR) repair [91].

Intracellular signaling. Following the aforementioned initial responses to high dose radiation (2–5 Gy), Trp53 protein, which is a nuclear protein, is phosphorylated by nuclear kinases, such ATM and DNA-PK, in cells of the post-pubertal BALB/c mouse mammary ducts and human tissue xenografts after 1 h and is redistributed to cytoplasm in luminal cells at 4–6 h whereas it remains in the nucleus in basal cells [91, 94–96]. Trp53 may induce apoptosis and cell cycle arrest, the latter possibly being regulated in parallel by Brca2 [97].

Gene expression. Activation of Trp53 as mentioned above induces expression of Cdkn1a (p21) in BALB/c mouse mammary ducts and lobuloalveoli [96].

Cell cycle regulation. An acute high dose (2–5 Gy) irradiation drastically decreases incorporation of bromodeoxyuridine (BrdU) in TEB of hybrid mice of C57BL/6 and BALB/cJ strains and Sprague–Dawley rats by 6 h, indicating induction of S phase arrest [97, 98]. In BALB/c mice, most basal and luminal cells show reduced Ki67-positive fractions after acute 6 Gy irradiation, implying entrance to G0, while a subset of proliferative basal mammary cells exhibit G2 arrest [92]. In Sprague–Dawley rats, release from cell cycle arrest occurs in basal cells by 24 h, when luminal cells show longer arrest [93].

Cell death. An acute high dose (2–5 Gy) irradiation induces only moderate apoptosis in mammary glands of post-pubertal BALB/c mice, hybrid mice of C57BL/6 and BALB/cJ strains and Sprague–Dawley rats [93–96]; this was Trp53-dependent in mice [96, 97] and observed also in adult BALB/c mice [98]. Apoptosis was more prominent in luminal than basal cells in BALB/c mice [92] and Sprague–Dawley rats [93]. At high doses (e.g. 4 Gy), reproductive cell death was more prominently induced in basal than luminal progenitor cells of Sprague–Dawley rats, whereas the effects were comparable at lower doses (e.g. 1 Gy) [93] (Fig. 4). In consistence, the percentage of basal cells decreased in BALB/c mice at 48 h after irradiation at 4 Gy [99]. Thus, importantly, acute high-dose exposure is more likely to induce imbalance between basal and luminal cells than chronic low-dose-rate exposure.

Intercellular signaling Evidence obtained with BALB/c mice suggests that activation of Trp53 after an acute high dose (5 Gy) exposure requires external TGFβ signaling activated by the ovarian hormones estrogen and progesterone [94, 95, 100]. Another line of evidence suggests stromal TGFβ is also required for various radiation-induced cancer-promoting effects, including the epithelial-mesenchymal transition, microenvironmental changes permissive for mammary stem cell activity and tumor formation and induction of stem cell-like status in epithelial cells (i.e. expression of both basal and luminal markers), all of which show a 'switch-like' (or all-or-none) dose response having a very low threshold below 100 mGy [101–103]. Such switch-like dose response can be a basis for dose rate effect.

Alteration of physiology and homeostasis. Acute high dose exposure (2 Gy) induced increased cell proliferation in post-pubertal Sprague–Dawley rats and C57BL/6 J mice [104, 105]. In mice, this long-term effect was attributed to elevation of blood estrogen, activation of the PI3K-Akt pathway and gene expression changes in the mammary epithelium [105, 106].

Development of premalignant lesions. Acute single irradiation at a high dose (2 Gy) induced hyperplastic changes in TEBs of the Sprague–Dawley rat mammary gland after 8 weeks [104].

Digestive system

The digestive system comprises organs that extend from the mouth to the anus covered by epithelial cells. These organs of the digestive system consist of the gastrointestinal tract (stomach, duodenum, jejunum, ileum, colon and rectum), aerodigestive tract (oral cavity and pharynx), esophagus and anal canal [107]. There is sufficient evidence that ionizing radiation has a carcinogenic effect on the gastrointestinal tract in human [88]. The tissue weighting factors of colon and stomach is 0.12, and esophagus is 0.04 [4] whereas the risk of radiation-induced cancer of the mouth and small intestine is extremely smaller than in these organs, so they are included in remainder tissues. The difference in susceptibility to cancer between small and large intestine could suggest that region-dependent tissue metabolism could affect dose-rate-effects, although the animal experiments on the dose-rate effects on the gastrointestinal tract are limited. In this section, we mainly describe the dose-rate effects on small and large intestine, for which informative results have been reported from several animal experiments.

Table 3. Mammary carcinogenesis studies comparing the effects of acute and chronic exposures

I.Fractionation

Species (strain)	Radiation	Effect measure	Acute exposure dose response	Dose per fraction (interval time)	Exposure period	Total dose (Gy)	Age when exposure started	Effect, fractionated	Effect, acute single	Reference
Mouse (BALB/c)	γ, ^{137}Cs	% with tumor (age-adjusted)	Linear-quadratic	10 mGy (1 d) 50 mGy (1 d)	25 d 5 d	0.25	12 wk	0.2%[a] 9.7%	12.3%	[77]
Rat (Sprague–Dawley)	γ, ^{60}Co	Increase in tumor no.	Linear	0.14–1.1 Gy (0.5 wk)	2–16 wk	4.4	6 wk	3–6/10^3 MD[b]	2–3/10^3 MD	[78, 79]
Rat (WAG/Rij)	X	Time to detection	Not analyzed	0.2 Gy (1 mo)	10 mo	2.0	8 wk	143 wk[c]	139 wk	[81]
Rat (WAG/Rij)	γ, ^{137}Cs	Excess normalized risk	Linear	2.5–10 mGy (0.5 d)	8–56 wk	1 or 2	8 wk	0.9–1.2/Gy[d]	1.1/Gy	[82, 84]
Rat (WAG/Rij), estrogen-treated	γ, ^{137}Cs	Excess normalized risk	Sigmoid	2.5–40 mGy (0.5 d)	2–56 wk	1 or 2	8 wk	0.6–2.4/Gy[d]	7.7 at 1 Gy[e]	[83, 84]

II. Continuous

Species (strain)	Radiation	Effect measure	Acute exposure dose response	Dose rate	Exposure period	Total dose (Gy)	Age when exposure started	Effect, continuous	Effect, acute single	Reference
Mouse (BALB/c)	γ, ^{137}Cs	% with tumor (age-adjusted)	Linear	0.069 mGy/min	6–24 d	0.5–2.0	10 wk	3.5%/Gy[f]	6.7%/Gy	[78]
Mouse (BALB/c)	γ, ^{137}Cs	% with tumor (age-adjusted)	Linear-quadratic	0.069 mGy/min	25 d	0.25	12 wk	−0.2%[a]	12.3%	[77]
Rat (Sprague–Dawley)	γ, ^{60}Co	No. of tumors (340 d after exposure)	Linear	0.03 R/min	2–18 d	0.8–7	'Young'	0.05/rat·Gy[g]	0.16/rat·Gy	[85][h]
Rat (Sprague–Dawley)	X, 200 kVp	No. of tumors (age 300 d)	Linear	0.02–0.14 mGy/min	10 d	0.29–2	7 wk	0.09/rat·Gy[g]	0.09/rat·Gy	[86, 87]
Rat (Sprague–Dawley)	γ, ^{60}Co	No. of tumors (age 300 d)	Linear	0.13 mGy/min	3–19 d	0.59–3.4	7 wk	0.00/rat·Gy[g] (≤2.3 Gy)	0.08/rat·Gy (≤2 Gy)	[86]
Rat (WAG/Rij)	γ, ^{60}Co	% with tumor (age 300 d)	Linear	0.07–0.22 mGy/min	13 d	1.3–4.1	11–13 wk	2.6%/Gy[f]	6.4%/Gy	[88][h]
Rat (Sprague–Dawley)	γ, ^{137}Cs	Hazard ratio	Linear	0.05–0.4 mGy/min 1 mGy/min	7–56 d 2.8 d	4.0 4.0	7 wk 7 wk	0.7–1.6 4.9	5.6 (13 wk)	[76]
Rat (Sprague–Dawley)	γ, ^{137}Cs	Hazard ratio	Linear	0.1 mGy/min	7–56 d	1.0–8.0	3 wk 7 wk	0.39/Gy 0.11/Gy	1.33/Gy (3–13 wk)	[76]

[a]Exposure-associated increase in percentage of animals with tumor (calculated from data in reference). [b]Exposure-associated increase in number of tumors per day per animal (calculated from data in reference). MD, mouse day. [c]Weeks of age when 50% of animals had a tumor (read from data in reference). [d]Increase per Gy in 'excess normalized risk' (value similar to excess relative risk as defined in reference). [e]Excess normalized risk at 1 Gy. [f]Increase per Gy in percentage of animals with tumor (calculated from data in reference). [g]Increase per Gy in number of tumors per animal (calculated from data in reference). [h]Articles other than peer-reviewed original papers. d, day; mo, month; wk, week.

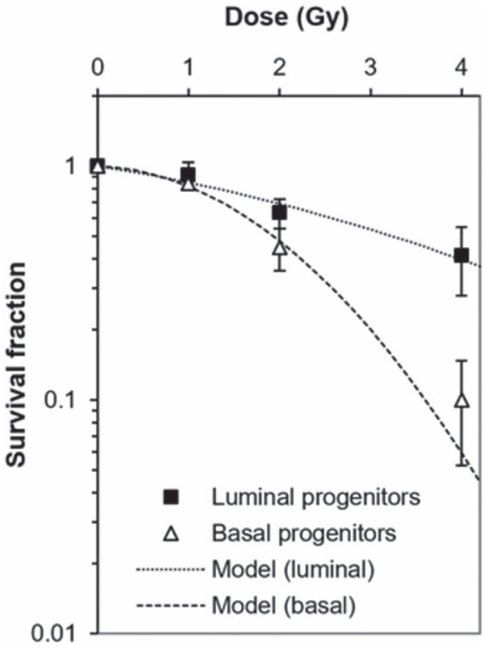

Fig. 4. Reproductive cell death of different mammary epithelial progenitors in rat mammary gland. Flow-sorted rat mammary epithelial cells were irradiated with γ-rays and colony formation was assessed. Adapted from Kudo *et al.* [93] (© 2023 Radiation Research Society).

Architecture, development and maintenance. General features of the digestive tract were well reviewed in ICRP 2012 [107]. Briefly, the stomach is a large muscular organ connecting the esophagus at the cardia and the small intestine at the pyloric sphincter in the gastrointestinal tract. The volume of the stomach was assumed to be 30 cm^3 and 175 cm^3 in human newborns and adults, respectively [108]. The gastric epithelium is a single layer of cells continuing with the basal layer of the stratified epithelium of the esophagus. Differentiated epithelial cells within gastric pits secrete hydrochloric acid, digestive enzymes and mucus [107]. In the mouse pyloric stomach, Leucine-rich repeat-containing G-protein coupled receptor 5 (Lgr5) was identified as a marker for self-renewing multipotent stem cells responsible for the long-term renewal of the gastric epithelium [109], as well as in the small and large intestine [110]. Recently, the membrane protein aquaporin 5 (AQP5) was identified as a marker that enriched for not only mouse but human adult pyloric stem cells [111]. $AQP5^+$ stem cells exist in the pyloric gland bases. In addition, $AQP5^+$ cells are source of gastric cancer, and $AQP5^+$ tumor cells show *ex vivo* stemness.

Structural and cellular features of the intestine have been thoroughly described in ICRP (2012) [107] and Hendry and Otsuka [112] (Fig. 5). Epithelial cells are continuingly generated from intestinal stem cells in the crypts, migrate upward along the crypt–villus axis and are eliminated by apoptosis at the tip of the villi, with a turnover time of 4–5 days in mice [113]. The cell-cycle time for the majority of proliferating cells may be of the order of 12–13 h, and the time for crypt stem cells is longer at approximately 24 h in mice [107]. The cell cycle time in the human intestine is in the order of 30 and 39 h for the colon and the rectum, respectively. The stem cell cycle in human colonic crypts is stated as approximately 36 h [112–114]. It was estimated that there are $\sim 5 \times 10^7$ crypts in the small intestine in man [114]. The length of the small intestine is ~270 cm, the diameter is about 2 cm and the surface area is ~1620 cm^2. Therefore, the crypt density is $\sim 3 \times 10^4$ per cm^2. Crypt density in the colon may be 2×10^4 per cm^2 or even less. The human colon is ~110 cm long, the diameter is ~5 cm and the surface area is ~1650 cm^2. Thus, there are $< 3 \times 10^7$ crypts in the large intestine in man [107, 112]. Recent studies indicated that approximately six functional stem cells at the very base of each colonic crypt in mice [115] and approximately seven stem cells in humans [116].

Intestinal stem cells exist at the bottom of crypts. The small cycling cells between Paneth cells are known as crypt base columnar (CBC) cells [117], and the Lgr5 is one of the molecular markers for CBC cells. In the case of the intestinal crypts, $Lgr5^+$ CBCs generate Wnt producing Paneth cells [110]. $Lgr5^+$ CBCs in the crypt bottom are interspersed with Paneth cells supplying Wnt proteins to maintain adjacent $Lgr5^+$ CBCs. Paneth cells thus constitute the niche for $Lgr5^+$ stem cells in the small intestine [118]. The other various intestinal stem cell markers have been reported to indicate differences in the characteristics of stem cells, and this has been reviewed by Hendry and Otsuka [112]. Cells located at the 4^{th} position from the crypt base (P4) in the small intestine are the quiescent stem cells expressing B lymphoma Mo-MLV insertion region 1 homolog (Bmi1), homeodomain-only protein (Hopx), leucine-rich repeats and immunoglobulin-like domains protein 1 (Lrig1), and/or high level of sex determining region Y box 9 ($Sox9^{high}$). In addition, very few quiescent stem cells that express extremely mouse telomerase reverse-transcriptase (mTert) are extremely resistant to a high dose (10 Gy) of radiation and can reconstitute all cell types in the small intestine [119]. On the other hand, Lgr5-positive stem cells are resistant to 1 Gy of irradiation but sensitive to 10 Gy [110]. Intermediate filament keratin-19 (Krt19)-positive and Lgr5-negative cells also have been identified as radioresistant stem cells located above P4 in both the small intestine and colon [120]. Also, the molecular markers of CBC cells have been identified including olfactomedin 4 (Olfm4), achaete-scute family bHLH transcription factor 2 (Ascl2), $Sox9^{low}$, etc. in addition to Lgr5. Colorectal Lgr5-positive stem cells were more radiosensitive than small intestinal those [121].

Dose-rate effect. To discuss dose-rate effect accurately, informative data sets that have complete dose response information obtained for different dose rates are required. However, animal experiments of dose-rate effects on the gastrointestinal tract are limited (Table 4).

In the rat stomach, localized 300 kV X-irradiation with single and fractionated (two and five fractions given daily and in 4 weeks, which was called as subchronic exposure) doses was reported [122]. Between 4 and 40 weeks after irradiation subchronic radiation damage was observed which presented itself as atonic dilatation of the stomach, with a α/β value range of 4.8–5.3 Gy. In the five-fraction experiment a significant increase in tolerance amounting to 800 mGy/day for the acute effect and 400 mGy/day for the subchronic effect was observed when intervals were increased from 1 day to 1 week.

In the mouse small intestine, induction of apoptotic cell death by low doses of γ-rays was independent of dose-rate between 0.0027 and 4.5 Gy/min [123]. Some P4 stem cells are highly sensitive to apoptosis

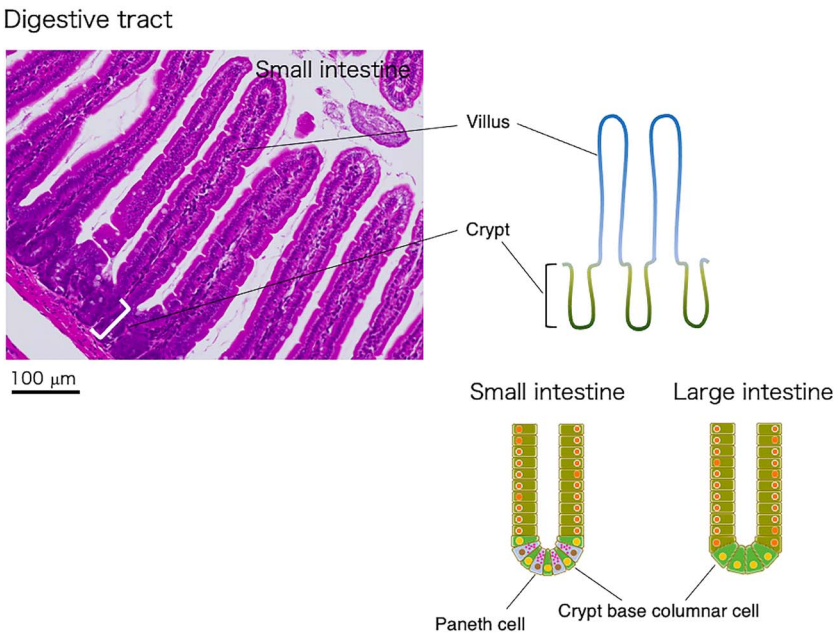

Fig. 5. Architecture of mouse intestine.

induced by radiation at doses as low as 100 mGy. The lack of a dose-rate effect may be due to the dose-rate used being so high that all of the stem cells were uniformly irradiated. However, these results suggest that during chronic irradiation, continuous deletion of damaged cells and their replacement may occur [88]. On the other hand, the fractionation effect of jejunal crypt survival after fractionated total body irradiation (TBI) of C3H mice given at 1.2 Gy/min was more valid than at 80 mGy/min [124]. The α/β value calculated by using linear-quadratic model was 13.3 Gy at 1.2 Gy/min and 96 Gy at 80 mGy/min, respectively. Recovery of cell survival by multifractionated irradiation with γ-rays was also reported in mouse (C3Hf/Bu) jejunal and colonic crypts [125, 126].

Under low dose-rate irradiation condition, any repair occur during irradiation, and therefore the extrapolation of the near-exponential portion of the crypt survival curve to zero dose, which was called back-extrapolation, could represent the pre-irradiation number of clonogens per crypt (clonogens were defined as cells that grow clonally). Additionally, the low dose-rate slope of the near-exponential portion could represent the αcomponent of a conventional linear-quadratic type survival curve [112]. In the *scid* mice having mutations on the *Prkdc* (DNA-dependent protein kinase catalytic subunit; DNA-PKcs), the α value was 0.74 ± 0.07 Gy^{-1}, compared to 0.22 ± 0.02 Gy^{-1} in the parental Balb/c mice, indicating that *scid* mice are ~3-fold more sensitive and the back-extrapolation was similar in both cases at a common value of 20 ± 6 [112, 127]. Therefore, clonogen radiosensitivity was increased about 3-fold higher by *scid* mutation, although the clonogen content per crypt was not different. Similar results were also obtained in the study using atm knockout mice [128]. In the *Atm*$^{-/-}$ mice, the back-extrapolation was 12 ± 6, and $\alpha = 0.60 \pm 0.10$ Gy^{-1}, compared to 13 ± 6 and $\alpha = 0.17 \pm 0.02$ Gy^{-1} in the parental wild-type FVB mice [112, 128]. Crypt survival in small intestine was also investigated using *Trp53* and *Bcl-2* knockout mice at 0.017 Gy/min (1 Gy/h) of ^{60}Co γ-rays [129]. Crypt survival levels were higher in *Trp53*$^{-/-}$ mice than in *Trp53*$^{+/+}$ and *Trp53*$^{+/-}$ mice after 25–30 Gy, but not after lower or higher doses. Similarly, crypt survival in *Bcl2*$^{-/-}$ mice was lower after all doses than *Bcl2*$^{+/+}$ and *Bcl2*$^{+/-}$ mice. These results suggest that the degree of curvature of the dose–response curve at a high dose-rate levels for some genotypes is not expected at lower dose-rate.

Lgr5^{+} stem cells in the mouse colon were much more radiosensitive than those in duodenum, because the number of colonic Lgr5^{+} stem cells decreased significantly after exposure to high dose-rate (0.5 Gy/min) X-rays at a dose 1 Gy [121]. Therefore, using the Lgr5-lineage tracing technique, the effects of low dose-rate (0.05 mGy/min) γ-rays on the replenishment of colonic Lgr5^{+} stem cells could be measured [130]. Unlike high dose-rate irradiation, which significantly promoted replenishment of Lgr5^{+} stem cells, no significant acceleration of stem cell replenishment was observed upon low-dose-rate irradiation.

Possible 'key events' related to dose rate effect in the digestive system Key events of the AOP related to the dose-rate effect, especially under low dose-rate irradiation condition, are not completely clear for the tissues/organs including digestive system. Therefore, the key events described below were mainly obtained by the studies using high dose and high dose-rate radiations. Importantly, a few recent studies have suggested that stem cell competition is one of the most important key events of the dose-rate effect in the intestine. For example, using stem cell-derived organoid culture system, irradiation at low dose-rates was shown to more efficiently eliminate damaged cells. Thus, the stem cell competition could provide a mechanism underlying the sparing effect of low-dose-rate irradiation [90].

DNA damage responses. The kinetics of 53BP1 foci formation, a surrogate marker for DSBs, has been studied in the mouse small intestine (duodenum and ileum) and colon irradiated with high dose-rate X-rays

Table 4. Summary of animal studies comparing the effects of acute and chronic exposures on digestive tract

Species (strain)	Part of irradiation	Analysis	Radiation source	Dose, dose rate	Effect, continuous or fractionated	Effect, acute single	Reference
Rat (Wistar) Female 3–6 M	Entire stomach	Survival, body weight, subchronic stomach dilatation	X, 300 kVp	10.7 and 21.3 Gy (single), 7.8–15.6 Gy (2 fractions), 3.6–9.9 Gy (5 fractions), 3 Gy/min	Survival 225 days after 2F/24 h[a] 142 days after 2F/4 weeks[b] 231 days after 5F/4 days[c] 181 days after 5F/4 weeks[d] Subchronic stomach dilatation (ED_{50}) 23.0 Gy (2F/24 h[a]) 20.3 Gy (2F/4 weeks[b]) 29.5 Gy (5F/4 days[c]) 39.9 Gy (5F/4 weeks[d])	Survival 70 days after irradiation Subchronic stomach dilatation (ED_{50}) 15.7 Gy	[122]
Mouse ($B6D2F_1$) Male 10–12 W	Whole body	Apoptotic cell death in the crypt	γ, ^{60}Co γ, ^{137}Cs X, 300 kVp n, 14.7 MeV n, 600 MeV	2.7, 5.3, 820 mGy/min 4.5 Gy/min 0.6 Gy/min 2.5, 5, 250 mGy/min 1, 3 mGy/min	Apoptotic cell death[e] No significant effect of dose-rate 2.7–4500 mGy/min (γ, ^{60}Co or ^{137}Cs) No significant effect of dose-rate 2.5–250 mGy/min (n, 14.7 MeV)		[123]
Mouse (C3H) Female 9–10 W	Whole body	Crypt cell survival	γ, ^{60}Co	0.02, 0.08, 0.36, 1.2, 4 Gy/min (1–20 fractions)	Crypt cell survival α/β = 96 Gy (0.08 Gy/min)	Crypt cell survival α/β = 13.3 Gy (1.2 Gy/min)	[124]
Mouse (C3Hf/Bu) 8–12 W	Whole body	Crypt cell survival	γ, ^{137}Cs	2.85 Gy/min (1–20 fractions)	Crypt cell survival D_0 = 1.75 Gy (2F, 9–12 Gy/F) D_0 = 2.23 Gy (3F, 6.25–9 Gy/F) D_0 = 2.83 Gy (5F, 4.2–6.3 Gy/F) D_0 = 3.34 Gy (10F, 2.8–4.4 Gy/F) D_0 = 4.21 Gy (15F, 1.9–3.2 Gy/F) D_0 = 4.05 Gy (20F, 1.55–2.55 Gy/F)	Crypt cell survival D_0 = 1.42 Gy (13.4–19.2 Gy)	[125]
Mouse (C3Hf/Bu) Female 8–12 W	Whole body	Crypt cell survival	γ, ^{60}Co n, 50 MeV n, 16 MeV	~ 1 Gy/min (20 fractions) 0.8–0.9 Gy/min (1–5 fractions) 0.25 Gy/min (1–5 fractions)	Crypt cell survival D_0 = 1.06 Gy (n, 50 MeV, 2F, 3.5–5 Gy/F) D_0 = 1.08 Gy (n, 50 MeV, 3F, 2.3–3.5 Gy/F) D_0 = 1.23 Gy (n, 50 MeV, 5F, 1.35–2.25 Gy/F) D_0 = 0.85 Gy (n, 16 MeV, 2F, 2.5–4 Gy/F) D_0 = 0.72 Gy (n, 16 MeV, 3F, 1.7–3.3 Gy/F) D_0 = 0.87 Gy (n, 16 MeV, 5F, 0.9–1.9 Gy/F)	Crypt cell survival D_0 = 0.93 Gy (n, 50 MeV, 6.5–10 Gy) D_0 = 0.81 Gy (n, 16 MeV, 4–10 Gy)	[136]

(*Continued*)

Table 4. Continued

Species (strain)	Part of irradiation	Analysis	Radiation source	Dose, dose rate	Effect, continuous or fractionated	Effect, acute single	Reference
Mouse (BALB/c, C.B-17/*scid*) 10–12 W	Whole body	Crypt cell survival	γ, ^{60}Co	16, 600 mGy/min	Crypt cell survival *scid* $\alpha = 0.74 \pm 0.07$ (Gy^{-1}) BALB/c $\alpha = 0.22 \pm 0.02$	Crypt cell survival *scid* $\alpha/\beta = 4.9 \pm 4.5$ ($\alpha = 0.50 \pm 0.24$ (Gy^{-1}), $\beta = 0.10 \pm 0.05$ (Gy^{-2})) BALB/c $\alpha/\beta = 4.3 \pm 4.7$ ($\alpha = 0.14 \pm 0.11$ (Gy^{-1}), $\beta = 0.032 \pm 0.010$ (Gy^{-2}))	[127]
Mouse (FVB/atm KO)	Whole body	Crypt cell survival	γ, ^{60}Co	0–40 Gy (17 mGy/min (= 1 Gy/h))	Crypt cell survival atm KO $\alpha = 0.60 \pm 0.10$ (Gy^{-1}) FVB $\alpha = 0.17 \pm 0.02$ (Gy^{-1})	-	[128]
Mouse (129Sv/C57BL/6/Trp53 KO, C57BL/6/bcl-2 KO, B6D2F$_1$) 10–12 W	Whole body	Crypt cell survival	γ, ^{60}Co	0–45 Gy (17 mGy/min (= 1 Gy/h))	Crypt cell survival Trp53$^{+/+}$ $\alpha = 0.13 \pm 0.02$ (Gy^{-1}) Trp53$^{+/-}$ $\alpha = 0.090 \pm 0.010$ (Gy^{-1}) Trp53$^{-/-}$ $\alpha = 0.031 \pm 0.007$ (Gy^{-1}) Bcl-2$^{+/+}$ $\alpha = 0.14 \pm 0.02$ (Gy^{-1}) Bcl-2$^{+/-}$ $\alpha = 0.19 \pm 0.03$ (Gy^{-1}) Bcl-2$^{-/-}$ $\alpha = 0.19 \pm 0.02$ (Gy^{-1}) B6D2F$_1$ $\alpha = 0.15 \pm 0.01$ (Gy^{-1})	-	[129]
Mouse (Lgr5-EGFP-IRES-CreERT2 × ROSA26-LSL-LacZ) 1 M	Whole body	Stem cell replacement (Lgr5 lineage tracing)	X, 260 kVp γ, ^{137}Cs	1 Gy (0.5 Gy/min) 1 Gy (0.05 mGy/min)	Colonic LacZ$^+$ crypts (%) 2.05 ± 0.79 (Sham) 1.78 ± 0.73 (1 Gy, 0.05 mGy/min)	Colonic LacZ$^+$ crypts (%) 1.98 ± 0.55 (Sham) 1.40 ± 0.06 (1 Gy, 0.5 Gy/min)	[130]

[a] 2 fractions (2F) in 24 h. [b] 2F given with 4 weeks interval. [c] 5F in 4 days. [d] 5F in given with 4 weeks interval. [e] incidence of apoptotic bodies in crypt section [123]. KO, knockout.

at doses 0.1, 1 or 4 Gy [131]. In the small intestine and colon, 53BP1 foci were similarly detected immediately after irradiation, but rapidly disappeared thereafter, especially noticeably in $Lgr5^+$ stem cells. In contrast, the colon was more susceptible to radiation-induced formation of 53BP1 foci. Additionally, the formation of γ-H2AX, BRCA1, RAD51 and phospho-DNA-PKcs at T2609 foci was studied in the mouse small intestinal CBC cells [132]. CBCs are relatively radioresistant, repairing DNA by HR significantly more efficiently than transit amplifying progenitors or villus cells. On the other hand, radiosensitivity of intestinal clonogens was increased in the Prkdc-mutated *scid* mice and Atm knockout mice [112, 127, 128]. The DNA repair kinetics is also different between CBCs and the $Lgr5^+$ mouse colonic epithelial stem cells (CESCs). After 19 Gy of whole body irradiation with high dose-rate (1.72 Gy/min) of γ-rays, CBCs and CESCs resolved γ-H2AX foci at different rates with CBCs repairing DSBs more slowly, a difference that persisted until at least 18 h after irradiation, a time at which CESCs had fully recovered [133].

Intracellular signaling. Nuclear factor-erythroid 2–related factor 2 (Nrf2) is a key transcriptional regulator of genes encoding antioxidant and anti-inflammation enzymes that binds to its endogenous inhibitor protein, Kelch-like ECH (erythroid cell-derived protein with CNC homology)-associated protein 1 (KEAP-1), in the cytoplasm. Upon irradiation, Nrf2 is translocated from the cytoplasm into the nucleus to induce transcription of heme oxygenase-1 (HO-1) and other cytoprotective enzymes through binding to antioxidant responsive elements. Mice fed with 2-cyano-3,12-dioxooleana-1,9 (11)-dien-28-oic acid (CDDO)-ethyl amide (EA), which is the chemically modified derivative of the synthetic triterpenoid CDDO showed resistance to TBI at a dose of 7.5 Gy. Mice fed with CDDO-EA were also greatly protected from TBI-induced reduction in crypt size, number, cell density and villus length in both the colon and small intestine as well as the induction of apoptosis in colonic crypts [134]. Also, studies showing the importance of intracellular redox potential of glutathione in cell proliferation, cellular differentiation and cell death by apoptosis in intestinal epithelium were precisely reviewed [135], but its contribution to the dose-rate effect has not yet been well cleared.

Gene expression. The expression levels of Trp53 and Cdkn1a (p21) increased in a time- and dose-dependent manner in mouse small and large intestine after 8 Gy of high dose-rate irradiation with ^{137}Cs γ-rays (3.8 Gy/min) [136]. In the small intestine, both Trp53 and Cdkn1a expressions were observed throughout crypts with the greatest frequency of expression over the first 15 cell positions, which includes the stem cell population (positions 3 to 5 and their vicinity) and the proliferating, transit cell population (positions 5 to 15 and their vicinity). Interestingly, cells expressing Trp53 were primarily distributed toward the crypt base. Subdivision of the Trp53-positive cell population revealed that the cells with the strongest Trp53 immunoreactivity were positioned farther toward the crypt base, and their distribution was almost coincident with the frequency distribution of apoptotic cells. Cells that were either weakly or moderately immunoreactive for Trp53 were located toward the middle of the crypt and were nearly coincident with the distribution of Cdkn1a. In the large intestine, Trp53 and Cdkn1a were observed along the entire length of the colonic crypts, and, unlike in the small intestine, this expression was not only maintained but increased over 72 h. The expression of Cdkn1a was detected in the colonic epithelium up to 6 days after irradiation. The expression of Cdkn1a could not be clearly detected 4 h after irradiation at a dose of 0.3 Gy in both small and large intestine. Meanwhile, after 1 Gy of high dose-rate (1.5 Gy/min) X-irradiation, the expression levels of Cdkn1a (p21) and Mdm2 increased significantly in the colon, but not in the duodenum, suggesting that the p53-dependent DNA damage response preferentially occurs in the colon, while the expression of Bax increased significantly in both organs [121].

Cell cycle regulation. In crypts of the mouse small and large intestine, irradiation with 8 Gy of ^{137}Cs γ-rays (3.8 Gy/min) severely reduced thymidine incorporation [136]. The incorporation of thymidine was gradually recovered, however, it returned to the normal level by 72 h after irradiation. Cells re-entering the cell cycle (i.e. thymidine-labeled cells) were observed at a lower position in the crypts. Also, preferential cell loss in the lower crypt was observed in mouse colon irradiated with X-rays at a high dose rate (0.5 Gy/min) [131]. Considerable reduction of cell numbers and dramatic induction of mitosis were observed after low-dose (0.1 Gy) X-irradiation in the colon but not in the small intestine. In a study of using the 5-ethynyl-2-deoxyuridine (EdU) staining method, small intestinal CBCs began cycling 12 h after 19 Gy of whole-body irradiation at a high dose-rate (1.72 Gy/min) γ-rays and by 15 h, maximal division was reinstituted [133]. Interestingly, it was estimated that about 60% of the small intestinal CBCs have not completed DNA repair at the time cell division reinitiates [133]. On the contrary, mouse CESCs began to exit growth arrest at 24 h after irradiation, and recovered their cycling levels by 48 h [133]. The kinetics of γ-H2AX indicated that DSBs were repaired by 18 h, a time preceding the checkpoint recovery initiation.

Cell death. In mouse stomach irradiated with ^{137}Cs γ-rays (2.6 Gy/min), maximum numbers of apoptotic cells were observed in both antrum and corpus at 48 h after irradiation at doses greater than 12 Gy [140]. However, the number of apoptotic cells observed in the gastric epithelium was much lower than observed in the small intestine or colon after similar doses of radiation. The greatest numbers of apoptotic cells were observed at cell positions 5–6 in the antrum and cell positions 15–18 in the corpus.

Radiation-induced apoptotic cell death in the intestine has already been thoroughly reviewed [107, 112]. In both duodenal and colonic crypts, caspase-3 positive cells were observed 6 h after exposure to 1 Gy of high dose-rate X-rays (1.5 Gy/min), and TdT-mediated dUTP Nick End Labeling (TUNEL)-positive cells were detected 24 h after irradiation. The frequency of cleaved caspase-3 and TUNEL-positive crypts showed that the frequency of apoptotic cells in crypts increased after 1 Gy of X-irradiation in both duodenum and colon [121]. As described above, it was reported that induction of apoptotic cell death by low doses of γ-rays was independent of dose-rate between 0.0027 and 4.5 Gy/min in the mouse small intestine [123]. Crypt survival levels were higher in $p53^{-/-}$ mice than in $Trp53^{+/+}$ and $Trp53^{+/-}$ mice after 25–30 Gy [137], and crypt survival of $Bcl\text{-}2^{-/-}$ mice was lower after all doses than $Bcl\text{-}2^{+/+}$ and $Bcl\text{-}2^{+/-}$ mice [129]. Additionally, significant alteration in the expression level of 26 autophagy and 17 oxidative stress-related genes was induced in the mouse jejunal-ileal region of the small intestine after exposure to 2 Gy of high dose-rate γ-rays

(700 mGy/min) [138]. Immunoprobing of intestinal sections showed decreased autophagosome marker LC3-II in the intestinal epithelial cells after irradiation. The mitotic catastrophe in the small intestinal crypts was 8 times higher than in the colonic crypts at 48 h after 19 Gy of whole-body irradiation at a high dose-rate (1.72 Gy/min) γ-rays [133].

Intercellular signaling. Many kinds of modifiers of gastrointestinal toxicity mediated by radiation, including interleukins, growth factors and cytokines, have been reported and reviewed by ICRP (2012) [107] and Hendry and Otsuka [112], however those mitigators are beyond the scope of this review. In the intestine, Wnt/β-catenin signaling is essential for the renewal of the intestines [139]. Disruption of Wnt signaling led to an abrupt cessation of proliferation in intestinal crypts following unbated loss of intestinal tissue and often morbidity. Reciprocally, the Wnt co-agonist R-spondin could potently stimulate intestinal proliferation. Lgr5 is well known as one of the Wnt target genes. Although the negligible effect of Lgr5$^+$ intestinal stem cells loss during homeostasis [140], depletion of Lgr5$^+$ cells during radiation (10 Gy)-induced damage and subsequent repair caused catastrophic crypt loss and deterioration of crypt-villus architecture [141]. Reactive oxygen species (ROS) are also well known to act as the intercellular signaling molecules. As described above, alteration of oxidative stress-related genes, as well as autophagy-related genes, was induced in the mouse jejunal-ileal region of the small intestine after exposure to 2 Gy of high dose-rate γ-rays (0.7 Gy/min) [138]. Radiation exposure led to persistently increased oxidant production and decreased anti-oxidant gene expression leading to oxidative stress and activation of proliferative Phosphoinositide 3-kinase/protein kinase B (PI3K/Akt)) and mammalian target of rapamycin (mTOR) signaling.

Alteration of physiology and homeostasis. Chronic exposures at a dose rate of a few mGy per year indicate that every cell in the body will be hit by a track of radiation every few months. This then makes a hit stem cell, at any time, compete against surrounding non-hit stem cells with in a niche. ICRP (2015) [90] described that 'if the elemental dose affects that stemness, the hit cells will be preferentially lost by competition from the tissue stem cell niche.' And 'Hence, stem cell competition at the tissue levels an ample possibility for a DREF value larger than unity, as in the case of the current DDREF value used by ICRP.' Recently, the gene expression profiles of in the mouse colonic Lgr5$^+$ stem cells, which were harvested by cell sorting at 2 weeks after exposure to 1 Gy of high dose-rate X-rays (0.5 Gy/min) or low dose-rate (0.05 mGy/min) γ-rays, were analyzed to identify key molecules that determine the dose-rate effects on the stem cell pool by RNA-sequence [142]. In the Lgr5$^+$ stem cells irradiated with high dose-rate X-rays, pathways related to DNA damage response, cell growth, cell differentiation and cell death were upregulated. Interestingly, pathways related to apical junctions and extracellular signaling were upregulated in the colonic Lgr5$^+$ stem cells irradiated with low dose-rate γ-rays. Apical junctions are known to play an important role in the exclusion of transformed cells that are surrounded by normal epithelial cells through 'cell competition.' Therefore, cell competition, through apical junctions and extracellular ligands, might contribute to the dose-rate effect on Lgr5$^+$ cell replenishment.

However, it is very difficult to evaluate radiation-induced stem cell competition under low dose-rate irradiation conditions *in vivo*. Recently, an organoid, having a crypt–villus-like structure [143], have been generated from Lgr5$^+$ intestinal stem cells at high efficiency *in vitro*. The intestinal organoid reflected the intestinal epithelium *in vivo*, because it contained all types of differentiated cells of the epithelium. The organoid-forming efficiency of irradiated cells relative to that of unirradiated controls could be defined as the surviving fraction of stem cells. Enzymatically dissociated single crypt cells from the duodenum and jejunum of mice were irradiated with 7.25, 29, 101, 304, 1000, 2000 and 4000 mGy of high dose-rate (100–470 mGy/min) X-rays immediately after plating, and the number of organoids was counted on day 12 [144]. A significant decrease in the surviving fraction of stem cells at approximately 1000 mGy. In a more recent study, Fujimichi *et al.* [145] established a two-color organoid culture system by mixing stem cells expressing different fluorescent colors. To analyze stem cell competition, two-color organoids were formed by mixing high dose-rate (0.5 Gy/min) X-irradiated and non-irradiated intestinal stem cells. In the two-color organoids, irradiated stem cells at a dose 1 Gy exhibited a growth disadvantage, although the organoid-forming potential (OFP) of the irradiated cells alone did not differ significantly from that of non-irradiated cells. This suggested that irradiated stem cells may become losers by the stem cell competition with non-irradiated cells, although more studies are needed to assess the effects of lower doses and lower dose-rates.

Development of premalignant lesions. At 24 h after 19 Gy of whole body irradiation with high dose-rate (1.72 Gy/min) γ-rays, mitotic cells in both the small and large intestines showed aberrant mitoses including anaphase bridges, multipolar spindles, misaligned chromosomes and chromosomal lagging [133]. Aberrant mitotic figures in small intestinal crypts were 8-fold higher than in large intestinal crypts. Additionally, in the study using Lgr5^{DTR} mice, in which the diphtheria toxin receptor (DTR) is knocked into the endogenous Lgr5 locus, the crypts, deficient for Lgr5$^+$ cells, are competent to undergo hyperplasia upon loss of Apc [142]. It suggests that Lgr5$^-$ reserve intestinal stem cells are radiosensitive, and Lgr5$^+$ cells are crucial for robust intestinal regeneration following radiation exposure, but are dispensable for premalignant hyperproliferation.

SUMMARY

This review summarizes the studies on dose-rate effects and discusses the biological mechanisms underlying the effects. Although several *in vitro* and *in vivo* studies have been reviewed, information on dose-rate dependent DSB induction in animal experimental models is still limited. The review also outlined dose-rate effects and key events, which are often related to tissue/organ structure and tissue stem cells, for mammary gland and gastrointestinal tract, while the summary for another three tissue/organ, which are hematopoietic tissue, lung and liver, is provided in Part II.

ACKNOWLEDGMENTS

This work was conducted as a part of the activity of Planning and Acting Network for Low Dose Radiation Research (PLANET). We are grateful to the following members of the administration committee

and the working group of PLANET who are not the authors of the present work: Drs. Kotaro Ozasa, Toshiyasu Iwasaki, Kazuo Sakai, Takashi Sugihara, Junya Kobayashi, Hiroshi Tauchi, Hiroshi Yasuda and Shin-ichi Kudo. We thank Drs. Yoshiya Shimada, Kazuo Yoshida, Michiya Sasaki, Tetsuo Nakajima and Daisuke Iizuka for their insightful comments and support.

DATA AVAILABILITY

The data underlying this article will be shared on reasonable request to the corresponding author.

CONFLICT OF INTEREST

The authors confirm they have no conflicts of interest.

REFERENCES

1. UNSCEAR. Levels and effects of radiation exposure due to the nuclear accident after the 2011 great east-Japan earthquake and tsunami. *UNSCEAR 2013 Report. Volume I, Scientific Annex a*. New York: United Nations, 2013, 2014, 1–311.
2. Ozasa K. Epidemiological research on radiation-induced cancer in atomic bomb survivors. *J Radiat Res* 2016;57:i112–7.
3. Grant EJ, Brenner A, Sugiyama H *et al.* Solid cancer incidence among the life span study of atomic bomb survivors: 1958-2009. *Radiat Res* 2017;187:513–37.
4. ICRP 2007. The 2007 recommendations of ICRP. ICRP publication 103. *Ann ICRP* 2007;37:1–332.
5. Brooks AL, Hoel DG, Preston RJ. The role of dose rate in radiation cancer risk: evaluating the effect of dose rate at the molecular, cellular and tissue levels using key events in critical pathways following exposure to low LET radiation. *Int J Radiat Biol* 2016;92:405–26.
6. Ruhm W, Woloschak GE, Shore RE *et al.* Dose and dose-rate effects of ionizing radiation: a discussion in the light of radiological protection. *Radiat Environ Biophys* 2015;54:379–401.
7. Ruhm W, Azizova T, Bouffler S *et al.* Typical doses and dose rates in studies pertinent to radiation risk inference at low doses and low dose rates. *J Radiat Res* 2018;59:ii1-ii10.
8. Haley BM, Paunesku T, Grdina DJ *et al.* The increase in animal mortality risk following exposure to sparsely ionizing radiation is not linear quadratic with dose. *PLoS One* 2015;10:e0140989.
9. Tang FR, Loke WK, Khoo BC. Low-dose or low-dose-rate ionizing radiation-induced bioeffects in animal models. *J Radiat Res* 2017;58:165–82.
10. Paunesku T, Haley B, Brooks A *et al.* Biological basis of radiation protection needs rejuvenation. *Int J Radiat Biol* 2017;93:1056–63.
11. Paunesku T, Woloschak G. Reflections on basic science studies involving low doses of ionizing radiation. *Health Phys* 2018;115:623–7.
12. Preston RJ, Ruhm W, Azzam EI *et al.* Adverse outcome pathways, key events, and radiation risk assessment. *Int J Radiat Biol* 2021;97:804–14.
13. Ankley GT, Bennett RS, Erickson RJ *et al.* Adverse outcome pathways: a conceptual framework to support ecotoxicology research and risk assessment. *Environ Toxicol Chem* 2010;29:730–41.
14. Chauhan V, Beaton D, Hamada N *et al.* Adverse outcome pathway: a path towards better data consolidation and global co-ordination of radiation research. *Int J Radiat Biol* 2022;98:1694–703. https://doi.org/10.1080/09553002.2021.2020363.
15. Tollefsen KE, Alonzo F, Beresford NA *et al.* Adverse outcome pathways (AOPs) for radiation-induced reproductive effects in environmental species: state of science and identification of a consensus AOP network. *Int J Radiat Biol* 2022;98:1816–31. https://doi.org/10.1080/09553002.2022.2110317.
16. Helm JS, Rudel RA. Adverse outcome pathways for ionizing radiation and breast cancer involve direct and indirect DNA damage, oxidative stress, inflammation, genomic instability, and interaction with hormonal regulation of the breast. *Arch Toxicol* 2020;94:1511–49. https://doi.org/10.1007/s00204-020-02752-z.
17. Chauhan V, Sherman S, Said Z *et al.* A case example of a radiation-relevant adverse outcome pathway to lung cancer. *Int J Radiat Biol* 2021;97:68–84. https://doi.org/10.1080/09553002.2019.1704913.
18. UNSCEAR. Biological mechanisms of radiation actions at low doses. *UNSCEAR 2012 Report*. New York: United Nations, 2012, 2012, 1–35.
19. Valentin J. Low-dose extrapolation of radiation-related cancer risk. ICRP publication 99. *Ann ICRP* 2005;35:1–140.
20. NCRP. Implications of recent epidemiologic studies for the linear-nonthreshold model and radiation protection. *NCRP Commentary 27*. Bethesda, 2018.
21. UNSCEAR 2017. Principles and criteria for ensuring the quality of the committee's reviews of epidemiological studies of radiation exposure. *UNSCEAR 2017 Report, Annex A*. New York: United Nations, 2018.
22. Hamra GB, Richardson DB, Cardis E *et al.* Cohort profile: the international nuclear workers study (INWORKS). *Int J Epidemiol* 2016;45:693–9.
23. Leuraud K, Richardson DB, Cardis E *et al.* Risk of cancer associated with low-dose radiation exposure: comparison of results between the INWORKS nuclear workers study and the A-bomb survivors study. *Radiat Environ Biophys* 2021;60:23–39.
24. Stram DO, Sokolnikov M, Napier BA *et al.* Lung cancer in the Mayak workers cohort: risk estimation and uncertainty analysis. *Radiat Res* 2021;195:334–46.
25. Boice JD Jr, Quinn B, Al-Nabulsi I *et al.* A million persons, a million dreams: a vision of a national center of radiation epidemiology and biology. *Int J Radiat Biol* 2022;98:795–821.
26. NCRP 1980. Influence of Dose and Its Distribution in Time on Dose-Response Relationships for Low-LET radiations. *NCRP Report 64*. Bethesda, 1980.
27. National Academy of Sciences. BEIR (2006) Chapter 4 "Quantitative Studies in Experimental Tumorigenesis". *BEIR VII Phase 2*. Washington DC: National Academy Press, 2006.

28. Yamamoto O, Seyama T, Itoh H *et al.* Oral administration of tritiated water (HTO) in mouse. III: low dose-rate irradiation and threshold dose-rate for radiation risk. *Int J Radiat Biol* 1998;73:535–41.
29. Tran V, Little MO. Dose and dose rate extrapolation factors for malignant and non-malignant health endpoints after exposure to gamma and neutron radiation. *Radiat Environ Biophys* 2017;56:299–328.
30. Doi K, Kai M, Suzuki K *et al.* Estimation of dose-rate effectiveness factor for malignant tumor mortality: joint analysis of mouse data exposed to chronic and acute radiation. *Radiat Res* 2019;194:500–10.
31. Braga-Tanaka I 3rd, Tanaka S, Kohda A *et al.* Experimental studies on the biological effects of chronic low dose-rate radiation exposure in mice: overview of the studies at the Institute for Environmental Sciences. *Int J Radiat Biol* 2018;94:423–33.
32. NCRP 2005. Extrapolation of radiation-induced cancer risks from nonhuman experimental systems to humans. *NCRP Report No. 150*. Bethesda, 2005.
33. Storer JB, Mitchell TJ, Fry RJ. Extrapolation of the relative risk of radiogenic neoplasms across mouse strains and to man. *Radiat Res* 1988;114:331–53.
34. Carnes BA, Olshansly SJ, Grahn D. An interspecies prediction of the risk of radiation-induced mortality. *Radiat Res* 1988;149:487–92.
35. Carnes BA, Grahn D, Hoel D. Mortality of atomic bomb survivors predicted from laboratory animals. *Radiat Res* 2003;160:159–67.
36. Preston RJ. Integrating basic radiobiological science and epidemiological studies: why and how. *Health Phys* 2015;108:125–30.
37. NCRP 2015. Health Effects of Low Doses of Radiation: Perspectives on Integrating Radiation Biology and Epidemiology. *NCRP Commentary No. 24*. Bethesda, 2015.
38. Dutta S, Sengupta P. Men and mice: relating their ages. *Life Sci* 2016;152:244–8.
39. Sengupta P. The laboratory rat: relating its age with human's. *Int J Prev Med* 2013;4:624–30.
40. Ohmura Y, Kuniyoshi Y. A translational model to determine rodent's age from human foetal age. *Sci Rep* 2017;7:17248.
41. Rogakou EP, Boon C, Redon C *et al.* Megabase chromatin domains involved in DNA double-strand breaks in vivo. *J Cell Biol* 1999;146:905–16.
42. Paull TT, Rogakou EP, Yamazaki V *et al.* A critical role for histone H2AX in recruitment of repair factors to nuclear foci after DNA damage. *Curr Biol* 2000;10:886–95.
43. Blackford AN, Jackson SP. ATM, ATR, and DNA-PK: the trinity at the heart of the DNA damage response. *Mol Cell* 2017;66:801–17.
44. Bonner WM, Redon CE, Dickey JS *et al.* GammaH2AX and cancer. *Nat Rev Cancer* 2008;8:957–67.
45. Lobrich M, Shibata A, Beucher A *et al.* gammaH2AX foci analysis for monitoring DNA double-strand break repair: strengths, limitations and optimization. *Cell Cycle* 2010;9:662–9.
46. Suzuki K, Okada H, Yamauchi M *et al.* Qualitative and quantitative analysis of phosphorylated ATM foci induced by low-dose ionizing radiation. *Radiat Res* 2006;165:499–504.
47. Suzuki K, Nakashima M, Yamashita S. Dynamics of ionizing radiation-induced DNA damage response in reconstituted three-dimensional human skin tissue. *Radiat Res* 2010;174:415–23.
48. Rothkamm K, Lobrich M. Evidence for a lack of DNA double-strand break repair in human cells exposed to very low x-ray doses. *Proc Acad Natl Sci USA* 2003;100:5057–62.
49. Asaithamby A, Chen DJ. Cellular responses to DNA double-strand breaks after low-dose gamma-irradiation. *Nucleic Acids Res* 2009;37:3912–23.
50. Sugihara T, Murano H, Tanaka K. Increased γ-H2A.X intensity in response to chronic medium-dose-rate γ-ray irradiation. *PLoS One* 2012;7:e45320.
51. Ishizaki K, Hayashi Y, Nakamura H *et al.* No induction of p53 phosphorylation and few focus formation of phosphorylated H2AX suggest efficient repair of DNA damage during chronic low-dose-rate irradiation in human cells. *J Radiat Res* 2004;45:521–5.
52. Cao L, Kawai H, Sasatani M *et al.* A novel ATM/TP53/p21-mediated checkpoint only activated by chronic γ-irradiation. *PLoS One* 2014;9:e104279.
53. Bunting SF, Nussenzweig A. End-joining, translocations and cancer. *Nat Rev Cancer* 2013;13:443–54.
54. Goodhead DT. Fifth Warren K. Sinclair keynote address: issues in quantifying the effects of low-level radiation. *Health Phys* 2009;97:394–406.
55. Sage E, Shikazono N. Radiation-induced clustered DNA lesions: repair and mutagenesis. *Free Radic Biol Med* 2017;107:125–35.
56. Rube CE, Dong X, Kuhne M *et al.* DNA double-strand break rejoining in complex normal tissues. *Int J Radiat Oncol Biol Phys* 2008;72:1180–7.
57. Hudson D, Kovalchuk I, Koturbash I *et al.* Induction and persistence of radiation-induced DNA damage is more pronounced in young animals than old animals. *Aging* 2011;3:609–20.
58. Schanz S, Schuler N, Lorat Y *et al.* Accumulation of DNA damage in complex normal tissues after protracted low-dose radiation. *DNA Repair* 2012;11:823–32.
59. Flokerzi E, Schanz S, Rube CE. Even low doses of radiation lead to DNA damage accumulation in lung tissue according to the genetically-defined DNA repair capacity. *Radiother Oncol* 2014;111:212–8.
60. Olipitz W, Wiktor-Brown D, Shuga J *et al.* Integrated molecular analysis indicates undetectable change in DNA damage in mice after continuous irradiation at ~400-fold natural background radiation. *Environ Health Perspect* 2012;120:1130–6.
61. UNSCEAR 2020/21. Biological mechanisms relevant for the inference of cancer risks from low-dose and low-dose-rate radiation. *UNSCEAR 2020/21 Report. Annex A*. New York: United Nations, 2021.
62. Brenner AV, Preston DL, Sakata R *et al.* Incidence of breast cancer in the life span study of atomic bomb survivors: 1958-2009. *Radiat Res* 2018;190:433–44.
63. Cardiff RD. Are the TDLU of the human the same as the LA of mice? *J Mammary Gland Biol Neoplasia* 1998;3:3–5.

64. Dontu G, Ince TA. Of mice and women: a comparative tissue biology perspective of breast stem cells and differentiation. *J Mammary Gland Biol Neoplasia* 2015;20: 51–62.
65. Fu NY, Nalan E, Linderman GJ *et al.* Stem cells and the differentiation hierarchy in mammary gland development. *Physiol Rev* 2019;100:489–523.
66. Navarrete MAH, Maier CM, Faloni R *et al.* Assessment of the proliferative, apoptotic and cellular renovation indices of the human mammary epithelium during the follicular and luteal phases of the menstrual cycle. *Breast Cancer Res* 2005;7:R306–13.
67. Schedin P, Mitrenga T, Maeck M. Estrous cycle regulation of mammary epithelial cell proliferation, differentiation, and death in the Sprague–Dawley rat: a model for investigating the role of estrous cycling in mammary carcinogenesis. *J Mammary Gland Biol Neoplasia* 2000;5:211–25.
68. Fata JE, Chaundhary V, Khokha R. Cellular turnover in the mammary gland is correlated with systemic levels of progesterone and not 17 beta-estradiol during the estrous cycle. *Biol Reprod* 2001;65:680–8.
69. Welm BE, Tepera SB, Venezia T *et al.* Sca-1(pos) cells in the mouse mammary gland represent an enriched progenitor cell population. *Dev Biol* 2002;245:42–56.
70. Imaoka T, Hisatsume H, Sakanishi Y *et al.* Progesterone stimulates proliferation of a long-lived epithelial cell population in rat mammary gland. *J Endocrinol Investig* 2011;35: 828–34.
71. Van Keymeulen A, Rocha AS, Ousset M *et al.* Distinct stem cells contribute to mammary gland development and maintenance. *Nature* 2011;479:189–93.
72. van Amerongen R, Bowman AN, Nusse R. Developmental stage and time dictate the fate of Wnt/β-catenin-responsive stem cells in the mammary gland. *Cell Stem Cell* 2012; 11:387–400.
73. Inskip PD, Robinson LL, Stovall M *et al.* Radiation dose and breast cancer risk in the childhood cancer survivor study. *J Clin Oncol* 2009;27:3901–7.
74. Imaoka T, Nishimura M, Iizuka D *et al.* Pre- and postpubertal irradiation induces mammary cancers with distinct expression of hormone receptors, erbB ligands, and developmental genes in rats. *Mol Carcinog* 2011;50:539–52.
75. Imaoka T, Nishimura M, Daino K *et al.* Influence of age on the relative biological effectiveness of carbon ion radiation for induction of rat mammary carcinoma. *Int J Radiat Oncol Biol Phys* 2013;85:1134–40.
76. Imaoka T, Nishimura M, Daino K *et al.* Prominent dose-rate effect and its age dependence of rat mammary carcinogenesis induced by continuous gamma-ray exposure. *Radiat Res* 2019;191:245–54.
77. Ullrich RL, Jernigan MC, Bowles ND. Radiation carcinogenesis: time-dose relationships. *Radiat Res* 1987;111:179–84.
78. Ullrich RL, Storer JB. Influence of gamma irradiation on the development of neoplastic disease in mice. III. Dose-rate effects. *Radiat Res* 1979;80:325–42.
79. Shellabarger CJ, Bond VP, Aponte GE *et al.* Results of fractionation and protraction of total-body radiation on rat mammary neoplasia. *Cancer Res* 1966;26:509–13.
80. Shellabarger CJ, Bond VP, Cronkite EP. Studies on radiation-induced mammary gland neoplasia in the rat. VII. The effects of fractionation and protraction of sublethal total-body irradiation. *Radiat Res* 1962;17:101–9.
81. Broerse JJ, Hennen LA, van Zwieten MJ. Radiation carcinogenesis in experimental animals and its implications for radiation protection. *Int J Radiat Biol Relat Stud Phys Chem Med* 1985;48:167–87.
82. Bartstra RW, Bentvelzen PA, Zoetelief J *et al.* Induction of mammary tumors in rats by single-dose gamma irradiation at different ages. *Radiat Res* 1998a;150:442–50.
83. Bartstra RW, Bentvelzen PA, Zoetelief J *et al.* The influence of estrogen treatment on induction of mammary carcinoma in rats by single-dose gamma irradiation at different ages. *Radiat Res* 1998b;150:451–8.
84. Bartstra RW, Bentvelzen PA, Zoetelief J *et al.* The effects of fractionated gamma irradiation on induction of mammary carcinoma in normal and estrogen-treated rats. *Radiat Res* 2000;153:557–69.
85. Shellabarger CJ, Brown RD. Rat mammary neoplasia following irradiation at 0.03 R or 10 R per minute. *Radiat Res* 1972;51:493–4.
86. Johnson JR, Gragtmans NJ, Myers DK *et al.* Dose-rate effects of mammary tumor development in female Sprague–Dawley rats exposed to X and gamma radiation. *Radiat Res* 1989;118:545–58.
87. Gragtmans NJ, Myers DK, Johnson JR *et al.* Occurrence of mammary tumors in rats after exposure to tritium beta rays and 200-kVp X rays. *Radiat Res* 1984;99:636–50.
88. Vogel JJ Jr, Dickson HW. Mammary neoplasia in Sprague–Dawley rats following acute and protracted irradiation. Broerse JJ, Gerber GB (eds). *Neutron Carcinogenesis*. Luxembourg: European Commission, 1982, 135–54.
89. Huper G, Marks JR. Isogenic normal basal and luminal mammary epithelial cells isolated by a normal method show a differential response to ionizing radiation. *Cancer Res* 2007;67: 2990–3001.
90. Niwa O, Barcellos-Hoff MH, Globus RK *et al.* ICRP publication 131: stem cell biology with respect to carcinogenesis aspects of radiological protection. *Ann ICRP* 2015;44:7–357.
91. Coates PJ, Appleyard MV, Murray K *et al.* Differential contextual responses of normal human breast epithelium to ionizing radiation in a mouse xenograft model. *Cancer Res* 2010;70: 9808–15.
92. Chang C-H, Zhang M, Rajapakshe K *et al.* Mammary stem cells and tumor-initiating cells are more resistant to apoptosis and exhibit increased DNA repair activity in response to DNA damage. *Stem Cell Rep* 2015;5:378–91.
93. Kudo KI, Takabatake M, Nagata K *et al.* Flow cytometry definition of rat mammary epithelial cell populations and their distinct radiation responses. *Radiat Res* 2020;194: 22–37.

94. Kuperwasser C, Pinkas J, Huribut GD *et al.* Cytoplasmic sequestration and functional repression of p53 in the mammary epithelium is reversed by hormonal treatment. *Cancer Res* 2000;60:2723–9.
95. Ewan KB, Henshall-Powell RL, Ravani SA *et al.* Transforming growth factor-beta1 mediates cellular response to DNA damage in situ. *Cancer Res* 2002;62:5627–31.
96. Minter LM, Dickinson ES, Naber SP *et al.* Epithelial cell cycling predicts p53 responsiveness to gamma-irradiation during post-natal mammary gland development. *Development* 2002;129:2997–3008.
97. Houle CD, Peddada SD, McAllister KA *et al.* Mutant Brca2/p53 mice exhibit altered radiation responses in the developing mammary gland. *Exp Toxicol Pathol* 2005;57:105–15.
98. Meyn RE, Stephens LC, Mason KA *et al.* Radiation-induced apoptosis in normal and pre-neoplastic mammary glands in vivo: significance of gland differentiation and p53 status. *Int J Cancer* 1996;65:466–72.
99. Woodward WA, Chen MS, Behbod F *et al.* WNT/beta-catenin mediates radiation resistance of mouse mammary progenitor cells. *Proc Natl Acad Sci U S A* 2007;104:618–23.
100. Becker KA, Lu S, Dickinson ES *et al.* Estrogen and progesterone regulate radiation-induced p53 activity in mammary epithelium through TGF-beta-dependent pathways. *Oncogene* 2005;24:6345–53.
101. Andarawewa KL, Costes SV, Fernandez-Garcia I *et al.* Lack of radiation dose or quality dependence of epithelial-to-mesenchymal transition (EMT) mediated by transforming growth factor β. *Int J Radiat Oncol Biol Phys* 2011;79:1523–31.
102. Nguyen DH, Oketch-Rabah HA, Illa-Bochaca I *et al.* Radiation acts on the microenvironment to affect breast carcinogenesis by distinct mechanisms that decrease cancer latency and affect tumor type. *Cancer Cell* 2011;19:640–51.
103. Tang J, Fernandez-Garcia I, Vijayakumar S *et al.* Irradiation of juvenile, but not adult, mammary gland increases stem cell self-renewal and estrogen receptor negative tumors. *Stem Cells* 2014;32:649–61.
104. Imaoka T, Nishimura M, Nishimura Y *et al.* Persistent cell proliferation of terminal end buds precedes radiation-induced rat mammary carcinogenesis. *In Vivo* 2006;20:353–8.
105. Datta K, Hyduke DR, Suman S *et al.* Exposure to ionizing radiation induced persistent gene expression changes in mouse mammary gland. *Radiat Oncol* 2012;7:205.
106. Suman S, Johnson MD, Fornace AJ Jr *et al.* Exposure to ionizing radiation causes long-term increase in serum estradiol and activation of PI3K-Akt signaling pathway in mouse mammary gland. *Int J Radiat Oncol Biol Phys* 2012;84:500–7.
107. ICRP 2012. ICRP statement on tissue reactions/early and late effects of radiation in normal tissues and organs – threshold doses for tissue reactions in a radiation protection context. ICRP publication 118. *Ann ICRP* 2012;41:1–322.
108. ICRP 2006. Human alimentary tract model for radiological protection. ICRP publication 100. *Ann ICRP* 2006;36:25–327.
109. Barker N, Huch M, Kujala P *et al.* Lgr5(+ve) stem cells drive self-renewal in the stomach and build long-lived gastric units in vitro. *Cell Stem Cell* 2010;6:25–36.
110. Barker N, van Es JH, Kuipers J *et al.* Identification of stem cells in small intestine and colon by marker gene Lgr5. *Nature* 2007;449:1003–7.
111. Tan SH, Swathi Y, Tan S *et al.* AQP5 enriches for stem cells and cancer origins in the distal stomach. *Nature* 2020;578:437–43.
112. Hendry JH, Otsuka K. The role of gene mutations and gene products in intestinal tissue reactions from ionising radiation. *Mutat Res* 2016;770:328–39.
113. Van der Flier LG, Clevers H. Stem cells, self-renewal, and differentiation in the intestinal epithelium. *Annu Rev Physiol* 2009;71:241–60.
114. Potten CS, Hendry JH. *Radiation and Gut*. Amsterdam: Elsevier, 1995.
115. Kozar S, Morrissey E, Nicholson AM *et al.* Continuous clonal labeling reveals small numbers of functional stem cells in intestinal crypts and adenomas. *Cell Stem Cell* 2013;13:626–33.
116. Baker AM, Cereser B, Melton S *et al.* Quantification of crypt and stem cell evolution in the normal and neoplastic human colon. *Cell Rep* 2014;8:940–7.
117. Cheng H, Leblond CP. Origin, differentiation and renewal of the four main epithelial cell types in the mouse small intestine. V. Unitarian theory of the origin of the four epithelial cell types. *Am J Anat* 1974;141:537–61.
118. Sato T, van Es JH, Snippert HJ *et al.* Paneth cells constitute the niche for Lgr5 stem cells in intestinal crypts. *Nature* 2011;469:415–8.
119. Montgomery RK, Carlone DL, Richmond CA *et al.* Mouse telomerase reverse transcriptase (mTert) expression marks slowly cycling intestinal stem cells. *Proc Natl Acad Sci U S A* 2011;108:179–84.
120. Asfaha S, Hayakawa Y, Muley A *et al.* Krt19(+)/Lgr5(−) cells are radioresistant cancer-initiating stem cells in the colon and intestine. *Cell Stem Cell* 2015;16:627–38.
121. Otsuka K, Hamada N, Magae J *et al.* Ionizing radiation leads to the replacement and de novo production of colonic Lgr5(+) stem cells. *Radiat Res* 2013;179:637–46.
122. Breiter N, Sassy T, Trott KR. The effect of dose fractionation on radiation injury in the rat stomach. *Radiother Oncol* 1993;27:223–8.
123. Hendry JH, Potten CS, Chadwick C *et al.* Cell death (apoptosis) in the mouse small intestine after low doses: effects of dose-rate, 14.7 MeV neutrons, and 600 MeV (maximum energy) neutrons. *Int J Radiat Biol Relat Stud Phys Chem Med* 1982;42:611–20.
124. Huczkowski J, Trott KR. Dose fractionation effects in low dose rate irradiation of jejunal crypt stem cells. *Int J Radiat Biol Relat Stud Phys Chem Med* 1984;46:293–8.
125. Withers HR, Mason KA. The kinetics of recovery in irradiated colonic mucosa of the mouse. *Cancer* 1974;34:896–903.
126. Withers HR, Mason K, Reid BO *et al.* Response of mouse intestine to neutrons and gamma rays in relation to dose fractionation and division cycle. *Cancer* 1974;34:39–47.
127. Hendry JH, Jiang TN. Differential radiosensitising effect of the scid mutation among tissues, studied using high and low dose rates: implications for prognostic indicators in radiotherapy. *Radiother Oncol* 1994;33:209–16.

128. Hendry JH. Radiation-induced apoptosis and its role in tissue response. *Int Congr Ser* 2002;1236:415–21.
129. Hendry JH, Broadbent DA, Roberts SA *et al.* Effects of deficiency in p53 or bcl-2 on the sensitivity of clonogenic cells in the small intestine to low dose-rate irradiation. *Int J Radiat Biol* 2000;76:559–65.
130. Otsuka K, Iwasaki T. Effects of dose rates on radiation-induced replenishment of intestinal stem cells determined by Lgr5 lineage tracing. *J Radiat Res* 2015;56:615–22.
131. Otsuka K, Suzuki K. Differences in radiation dose response between small and large intestinal crypts. *Radiat Res* 2016; 186:302–14.
132. Hua G, Thin TH. Feldman R *et al* crypt base columnar stem cells in small intestines of mice are radioresistant. *Gastroenterology* 2012;143:1266–76.
133. Hua G, Wang C, Pan Y *et al.* Distinct levels of radioresistance in $Lgr5^+$ colonic epithelial stem cells versus $Lgr5^+$ small intestinal stem cells. *Cancer Res* 2017;77:2124–33.
134. Kim SB, Pandita RK, Eskiocak U *et al.* Targeting of Nrf2 induces DNA damage signaling and protects colonic epithelial cells from ionizing radiation. *Proc Natl Acad Sci U S A* 2012;109:E2949–55.
135. Pérez S, Taléns-Visconti R, Rius-Pérez S *et al.* Redox signaling in the gastrointestinal tract. *Free Radic Biol Med* 2017;104:75–103.
136. Wilson JW, Pritchard DM, Hickman JA, Potten CS. Radiation-induced p53 and p21WAF-1/CIP1 expression in the murine intestinal epithelium: apoptosis and cell cycle arrest. *Am J Pathol* 1998;153:899–909.
137. Przemeck SM, Duckworth CA, Pritchard DM. Radiation-induced gastric epithelial apoptosis occurs in the proliferative zone and is regulated by p53, bak, bax, and bcl-2. *Am J Physiol Gastrointest Liver Physiol* 2007;292:G620–7.
138. Datta K, Suman S, Fornace AJ Jr. Radiation persistently promoted oxidative stress, activated mTOR via PI3K/Akt, and downregulated autophagy pathway in mouse intestine. *Int J Biochem Cell Biol* 2014;57:167–76.
139. Clevers H, Loh KM, Nusse R. Stem cell signaling. An integral program for tissue renewal and regeneration: Wnt signaling and stem cell control. *Science* 2014;346:1248012.
140. Tian H, Biehs B, Warming S *et al.* A reserve stem cell population in small intestine renders Lgr5-positive cells dispensable. *Nature* 2011;478:255–9.
141. Metcalfe C, Kljavin NM, Ybarra R *et al.* Lgr5+ stem cells are indispensable for radiation-induced intestinal regeneration. *Cell Stem Cell* 2014;14:149–59.
142. Otsuka K, Suzuki K, Fujimichi Y *et al.* Cellular responses and gene expression profiles of colonic $Lgr5^+$ stem cells after low-dose/low-dose-rate radiation exposure. *J Radiat Res* 2018;59:ii18–22.
143. Sato T, Vries RG, Snippert HJ *et al.* Single Lgr5 stem cells build crypt-villus structures in vitro without a mesenchymal niche. *Nature* 2009;459:262–5.
144. Yamauchi M, Otsuka K, Kondo H *et al.* A novel in vitro survival assay of small intestinal stem cells after exposure to ionizing radiation. *J Radiat Res* 2014;55:381–90.
145. Fujimichi Y, Otsuka K, Tomita M, Iwasaki T. An efficient intestinal organoid system of direct sorting to evaluate stem cell competition in vitro. *Sci Rep* 2019;9: 20297.